Scaling of space–time modes with Reynolds number in two-dimensional turbulence

Nicholas Kevlahan

Department of Mathematics & Statistics

McMaster University

18 July 2006

Collaborators

- Jahrul Alam
  McMaster University (PhD student)
- Oleg Vasilyev
  University of Colorado at Boulder

Outline

Intermittency and turbulence

- The active regions of turbulence are distributed inhomogeneously in space and time.
- The active proportion of the flow is believed to decrease with Reynolds number.
- This intermittency is a fundamental property of turbulence.

Intermittency and turbulence

- The active regions of turbulence are distributed inhomogeneously in space and time.
- The active proportion of the flow is believed to decrease with Reynolds number.
- This intermittency is a fundamental property of turbulence.

Intermittency and turbulence

- The active regions of turbulence are distributed inhomogeneously in space and time.
- The active proportion of the flow is believed to decrease with Reynolds number.
- This intermittency is a fundamental property of turbulence.

Intermittency and turbulence

- The active regions of turbulence are distributed inhomogeneously in space and time.
- The active proportion of the flow is believed to decrease with Reynolds number.
- This intermittency is a fundamental property of turbulence.

Qualitative picture of intermittency

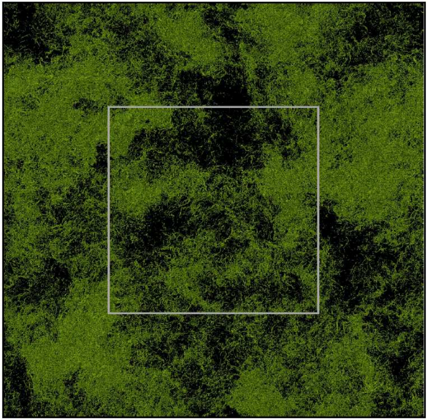

DNS of homogeneous isotropic turbulence at $\mathrm{Re}_\lambda = 1\,217$ (Yokokawa et al. 2002). Active regions are intermittent (and fractal?).

Qualitative picture of intermittency

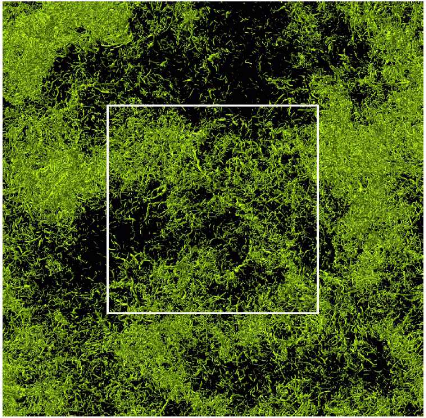

DNS of homogeneous isotropic turbulence at $\mathrm{Re}_\lambda = 1\,217$ (Yokokawa et al. 2002). Active regions are intermittent (and fractal?).

Qualitative picture of intermittency

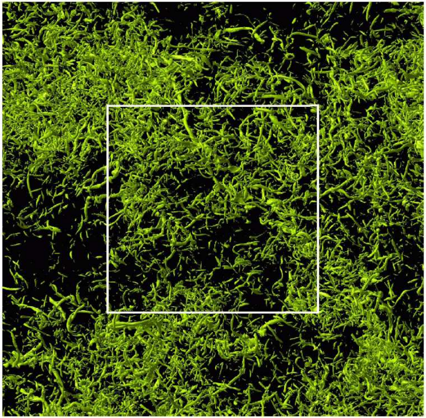

DNS of homogeneous isotropic turbulence at $\mathrm{Re}_\lambda = 1\,217$ (Yokokawa et al. 2002). Active regions are intermittent (and fractal?).

Qualitative picture of intermittency

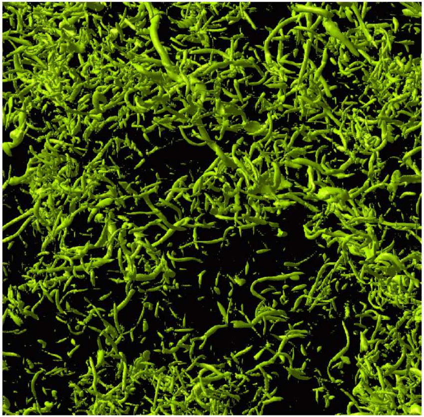

DNS of homogeneous isotropic turbulence at $\mathrm{Re}_\lambda = 1\,217$ (Yokokawa et al. 2002). Active regions are intermittent (and fractal?).

Mathematical estimates of number of turbulence modes

- Foias & Prodi (1967) conjectured that solutions of the Navier–Stokes equations are determined uniquely by a finite number of spatial modes.
- Friz & Robinson (2001) proved this conjecture for stationary periodic 2D turbulence.
- Jones & Titi (1993) found an upper bound on the number of spatial Fourier required to represent 2D periodic turbulence of $O(Re^2)$.
- Galdi (2006) extended this result to 3D flow past bluff bodies.

Mathematical estimates of number of turbulence modes

- Foias & Prodi (1967) conjectured that solutions of the Navier–Stokes equations are determined uniquely by a finite number of spatial modes.
- Friz & Robinson (2001) proved this conjecture for stationary periodic 2D turbulence.
- Jones & Titi (1993) found an upper bound on the number of spatial Fourier required to represent 2D periodic turbulence of $O(Re^2)$.
- Galdi (2006) extended this result to 3D flow past bluff bodies.

Mathematical estimates of number of turbulence modes

- Foias & Prodi (1967) conjectured that solutions of the Navier–Stokes equations are determined uniquely by a finite number of spatial modes.
- Friz & Robinson (2001) proved this conjecture for stationary periodic 2D turbulence.
- Jones & Titi (1993) found an upper bound on the number of spatial Fourier required to represent 2D periodic turbulence of $O(Re^2)$.
- Galdi (2006) extended this result to 3D flow past bluff bodies.

Mathematical estimates of number of turbulence modes

- Foias & Prodi (1967) conjectured that solutions of the Navier–Stokes equations are determined uniquely by a finite number of spatial modes.
- Friz & Robinson (2001) proved this conjecture for stationary periodic 2D turbulence.
- Jones & Titi (1993) found an upper bound on the number of spatial Fourier required to represent 2D periodic turbulence of $O(Re^2)$.
- Galdi (2006) extended this result to 3D flow past bluff bodies.

Mathematical estimates of number of turbulence modes

- Foias & Prodi (1967) conjectured that solutions of the Navier–Stokes equations are determined uniquely by a finite number of spatial modes.
- Friz & Robinson (2001) proved this conjecture for stationary periodic 2D turbulence.
- Jones & Titi (1993) found an upper bound on the number of spatial Fourier required to represent 2D periodic turbulence of $O(Re^2)$.
- Galdi (2006) extended this result to 3D flow past bluff bodies.

Computational complexity of turbulence simulations

- Assuming homogeneity, the spatial computational complexity of turbulence scales like $Re^{9/4}$ (or Re^{1} in 2D).
- Similarly, space–time computational complexity scales like Re^{3} (or $Re^{3/2}$ in 2D).
- Yakhot & Sreenivasan recently claimed it is even worse: Re^{4}.
- However, these estimates ignore intermittency.

Computational complexity of turbulence simulations

- Assuming homogeneity, the spatial computational complexity of turbulence scales like $Re^{9/4}$ (or Re^1 in 2D).
- Similarly, space–time computational complexity scales like Re^3 (or $Re^{3/2}$ in 2D).
- Yakhot & Sreenivasan recently claimed it is even worse: Re^4.
- However, these estimates ignore intermittency.

Computational complexity of turbulence simulations

- Assuming homogeneity, the spatial computational complexity of turbulence scales like $Re^{9/4}$ (or Re^1 in 2D).
- Similarly, space–time computational complexity scales like Re^3 (or $Re^{3/2}$ in 2D).
- Yakhot & Sreenivasan recently claimed it is even worse: Re^4.
- However, these estimates ignore intermittency.

Computational complexity of turbulence simulations

- Assuming homogeneity, the spatial computational complexity of turbulence scales like $Re^{9/4}$ (or Re^{1} in 2D).
- Similarly, space–time computational complexity scales like Re^{3} (or $Re^{3/2}$ in 2D).
- Yakhot & Sreenivasan recently claimed it is even worse: Re^{4}.
- However, these estimates ignore intermittency.

Computational complexity of turbulence simulations

- Assuming homogeneity, the spatial computational complexity of turbulence scales like $Re^{9/4}$ (or Re^{1} in 2D).
- Similarly, space–time computational complexity scales like Re^{3} (or $Re^{3/2}$ in 2D).
- Yakhot & Sreenivasan recently claimed it is even worse: Re^{4}.
- However, these estimates ignore intermittency.

Questions

- What is the actual scaling of spatial degrees of freedom with Reynolds number, Re^{β}?
- What is the actual scaling of space-time degrees of freedom with Reynolds number, Re^{α}?
- Is turbulence more intermittent in space or time?
- What is the fractal dimension of the active regions of the flow? (Assuming the β−model.)

Questions

- What is the actual scaling of spatial degrees of freedom with Reynolds number, Re^{β}?
- What is the actual scaling of space-time degrees of freedom with Reynolds number, Re^{α}?
- Is turbulence more intermittent in space or time?
- What is the fractal dimension of the active regions of the flow? (Assuming the β−model.)

Questions

- What is the actual scaling of spatial degrees of freedom with Reynolds number, Re^{β}?
- What is the actual scaling of space-time degrees of freedom with Reynolds number, Re^{α}?
- Is turbulence more intermittent in space or time?
- What is the fractal dimension of the active regions of the flow? (Assuming the $\beta-$model.)

Questions

- What is the actual scaling of spatial degrees of freedom with Reynolds number, Re^{β}?
- What is the actual scaling of space-time degrees of freedom with Reynolds number, Re^{α}?
- Is turbulence more intermittent in space or time?
- What is the fractal dimension of the active regions of the flow? (Assuming the $\beta-$model.)

Questions

- What is the actual scaling of spatial degrees of freedom with Reynolds number, Re^{β}?
- What is the actual scaling of space-time degrees of freedom with Reynolds number, Re^{α}?
- Is turbulence more intermittent in space or time?
- What is the fractal dimension of the active regions of the flow? (Assuming the $\beta-$model.)

Numerical estimation of space-time modes

- Use a simultaneous space–time adaptive wavelet solver.
- Take the number of active space–time wavelet modes as an upper bound on the number of space–time degrees of freedom.
- Consider periodic, unforced, 2D turbulence.
- Perform a sequence of simulations for $1\,260 \leq Re \leq 40\,400$.

Numerical estimation of space-time modes

- Use a simultaneous space–time adaptive wavelet solver.
- Take the number of active space–time wavelet modes as an upper bound on the number of space–time degrees of freedom.
- Consider periodic, unforced, 2D turbulence.
- Perform a sequence of simulations for $1\,260 \leq Re \leq 40\,400$.

Numerical estimation of space-time modes

- Use a simultaneous space–time adaptive wavelet solver.
- Take the number of active space–time wavelet modes as an upper bound on the number of space–time degrees of freedom.
- Consider periodic, unforced, 2D turbulence.
- Perform a sequence of simulations for $1\,260 \leq Re \leq 40\,400$.

Numerical estimation of space-time modes

- Use a simultaneous space–time adaptive wavelet solver.
- Take the number of active space–time wavelet modes as an upper bound on the number of space–time degrees of freedom.
- Consider periodic, unforced, 2D turbulence.
- Perform a sequence of simulations for $1\,260 \le Re \le 40\,400$.

Numerical estimation of space-time modes

- Use a simultaneous space–time adaptive wavelet solver.
- Take the number of active space–time wavelet modes as an upper bound on the number of space–time degrees of freedom.
- Consider periodic, unforced, 2D turbulence.
- Perform a sequence of simulations for $1\,260 \leq Re \leq 40\,400$.

Why use a wavelet basis for adaptivity?

- High rate of data compression (e.g. jpeg2 2000 image compression).
- Fast $O(\mathcal{N})$ transform.
- Fast signal de-noising (optimal for additive Gaussian noise).
- Easy to control wavelet properties (e.g. smoothness, boundary conditions).

Why use a wavelet basis for adaptivity?

- High rate of data compression (e.g. jpeg2 2000 image compression).
- Fast $O(\mathcal{N})$ transform.
- Fast signal de-noising (optimal for additive Gaussian noise).
- Easy to control wavelet properties (e.g. smoothness, boundary conditions).

Why use a wavelet basis for adaptivity?

- High rate of data compression (e.g. jpeg2 2000 image compression).
- Fast $O(\mathcal{N})$ transform.
- Fast signal de-noising (optimal for additive Gaussian noise).
- Easy to control wavelet properties (e.g. smoothness, boundary conditions).

Why use a wavelet basis for adaptivity?

- High rate of data compression (e.g. jpeg2 2000 image compression).
- Fast $O(\mathcal{N})$ transform.
- Fast signal de-noising (optimal for additive Gaussian noise).
- Easy to control wavelet properties (e.g. smoothness, boundary conditions).

Why use a wavelet basis for adaptivity?

- High rate of data compression (e.g. jpeg2 2000 image compression).
- Fast $O(\mathcal{N})$ transform.
- Fast signal de-noising (optimal for additive Gaussian noise).
- Easy to control wavelet properties (e.g. smoothness, boundary conditions).

Wavelet multiresolution analysis of $\mathbf{L}^2(\mathbb{R})$

A sequence of approximation subspaces
$\mathbf{M} = \{V^j \subset \mathbf{L}^2(\mathbb{R}) \mid j \in \mathcal{J}\}$ s.t.

- $V^j \subset V^{j+1}$ (subspaces are nested).
- $\cup_{j \in \mathcal{J}} V^j$ is dense in $\mathbf{L}^2(\mathbb{R})$.
- Each V^j has a Riesz basis of scaling functions $\{\phi^j_k \mid k \in \mathcal{K}^j\}$.

Wavelet multiresolution analysis of $\mathbf{L}^2(\mathbb{R})$

A sequence of approximation subspaces
$\mathbf{M} = \{V^j \subset \mathbf{L}^2(\mathbb{R}) \mid j \in \mathcal{J}\}$ s.t.

- $V^j \subset V^{j+1}$ (subspaces are nested).
- $\cup_{j\in\mathcal{J}} V^j$ is dense in $\mathbf{L}^2(\mathbb{R})$.
- Each V^j has a Riesz basis of scaling functions $\{\phi_k^j \mid k \in \mathcal{K}^j\}$.

Wavelet multiresolution analysis of $\mathbf{L}^2(\mathbb{R})$

A sequence of approximation subspaces
$\mathbf{M} = \{V^j \subset \mathbf{L}^2(\mathbb{R}) \mid j \in \mathcal{J}\}$ s.t.

- $V^j \subset V^{j+1}$ (subspaces are nested).
- $\cup_{j\in\mathcal{J}} V^j$ is dense in $\mathbf{L}^2(\mathbb{R})$.
- Each V^j has a Riesz basis of scaling functions $\{\phi_k^j \mid k \in \mathcal{K}^j\}$.

Wavelet multiresolution analysis of $\mathbf{L}^2(\mathbb{R})$

A sequence of approximation subspaces
$\mathbf{M} = \{V^j \subset \mathbf{L}^2(\mathbb{R}) \mid j \in \mathcal{J}\}$ s.t.

- $V^j \subset V^{j+1}$ (subspaces are nested).
- $\cup_{j\in\mathcal{J}} V^j$ is dense in $\mathbf{L}^2(\mathbb{R})$.
- Each V^j has a Riesz basis of scaling functions $\{\phi_k^j \mid k \in \mathcal{K}^j\}$.

Wavelet multiresolution analysis of $\mathbf{L}^2(\mathbb{R})$

A sequence of approximation subspaces
$\mathbf{M} = \{V^j \subset \mathbf{L}^2(\mathbb{R}) \mid j \in \mathcal{J}\}$ s.t.

- $V^j \subset V^{j+1}$ (subspaces are nested).
- $\cup_{j\in\mathcal{J}} V^j$ is dense in $\mathbf{L}^2(\mathbb{R})$.
- Each V^j has a Riesz basis of scaling functions $\{\phi_k^j \mid k \in \mathcal{K}^j\}$.

Wavelets ψ_k^j span the complement space W^j, where
$V^{j+1} = V^j \oplus W^j$, i.e. wavelet coefficients give the detail.

Nested collocation wavelet grids

Scaling functions are constructed from interpolating polynomials of degree $2N-1$ on nested grids:

$$\mathcal{G}^j = \left\{ x_k^j \in \Omega : \; x_k^j = x_{2k}^{j+1}, \; k \in \mathcal{K}^j \right\}$$

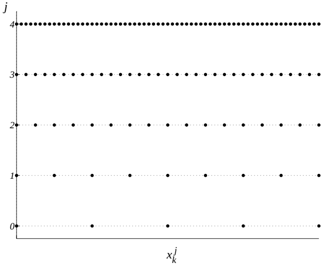

Collocation: each scaling function and wavelet is associated to a unique grid point.

Nested collocation wavelet grids

Scaling functions are constructed from interpolating polynomials of degree $2N-1$ on nested grids:

$$\mathcal{G}^j = \left\{ x_k^j \in \Omega : \; x_k^j = x_{2k}^{j+1}, \; k \in \mathcal{K}^j \right\}$$

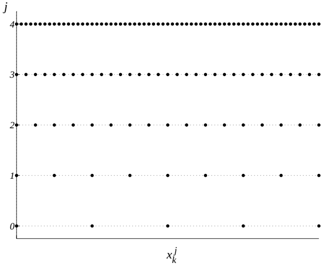

Collocation: each scaling function and wavelet is associated to a unique grid point.

$$u(x) = \sum_{k \in \mathcal{K}^J} u(x_k^J)\phi_k^J(x) = \sum_{k \in \mathcal{K}^0} u(x_k^0)\phi_k^0(x) + \sum_{j=0}^{J-1} \sum_{k \in \mathcal{L}^j} d_k^j \psi_k^j(x)$$

Wavelet compression

$$u(x) = \sum_{k\in\mathcal{K}^0} u(x_k^0)\phi_k^0(x) + \sum_{j=0}^{+\infty} \sum_{k\in\mathcal{L}^j} d_k^j \psi_k^j(x)$$

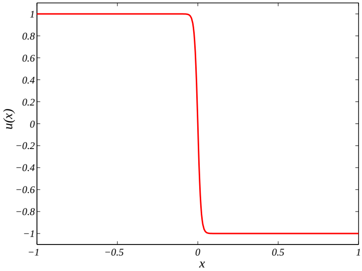

Function $u(x)$

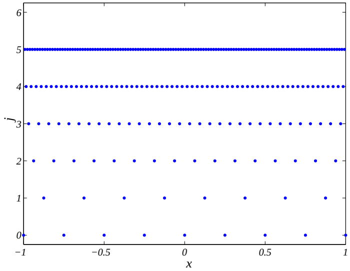

Wavelet locations x_k^j

Wavelet compression

$$u_{\geq}(x) = \sum_{k \in \mathcal{K}^0} u(x_k^0)\phi_k^0(x) + \sum_{j=0}^{J-1} \sum_{\substack{k \in \mathcal{L}^j \\ |d^j{}_k| \geq \epsilon}} d_k{}^j \psi_k{}^j(x)$$

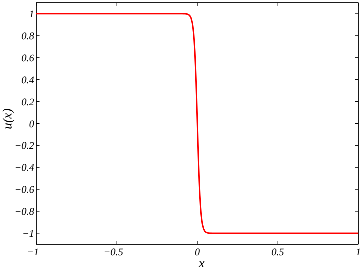

Function $u(x)$

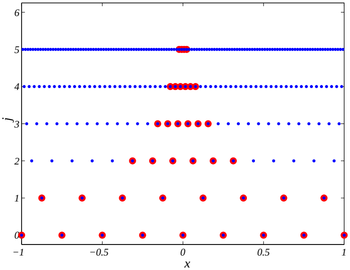

Wavelet locations $x_k{}^j$ $\epsilon = 10^{-3}$

Wavelet compression

$$\begin{aligned} ||u(x) - u_{\geq}(x)||_2 &= O(\epsilon) \\ \mathcal{N} &= O(\epsilon^{-1/2N}) \\ ||u(x) - u_{\geq}(x)||_2 &= O(\mathcal{N}^{-2N}) \end{aligned}$$

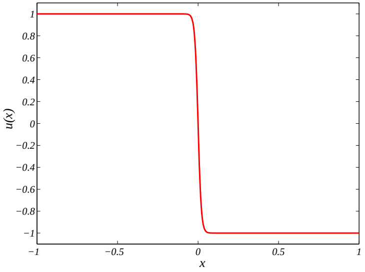

Function $u(x)$

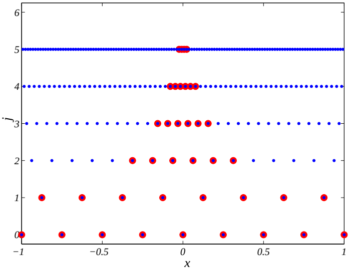

Wavelet locations x_k^j $\epsilon = 10^{-3}$

Space–time adaptive wavelet turbulence calculation

Advantages

Space–time adaptive wavelet turbulence calculation

Advantages

- Global error control in time.
- Local time step.
- Potentially optimal complexity for highly intermittent problems
- Number of grid points is an approximation to the number of space–time degrees of freedom in the flow.

Space–time adaptive wavelet turbulence calculation

Advantages

- Global error control in time.
  Error grows uncontrollably in classical time marching.
- Local time step.
- Potentially optimal complexity for highly intermittent problems
- Number of grid points is an approximation to the number of space–time degrees of freedom in the flow.

Space–time adaptive wavelet turbulence calculation

Advantages

- Global error control in time.
  Error grows uncontrollably in classical time marching.
- Local time step.
- Potentially optimal complexity for highly intermittent problems
- Number of grid points is an approximation to the number of space–time degrees of freedom in the flow.

Space–time adaptive wavelet turbulence calculation

Advantages

- Global error control in time.
  Error grows uncontrollably in classical time marching.
- Local time step.
- Potentially optimal complexity for highly intermittent problems
- Number of grid points is an approximation to the number of space–time degrees of freedom in the flow.

Space–time adaptive wavelet turbulence calculation

Advantages

- Global error control in time.
  Error grows uncontrollably in classical time marching.
- Local time step.
- Potentially optimal complexity for highly intermittent problems
- Number of grid points is an approximation to the number of space–time degrees of freedom in the flow.

Numerical method: pseudo BVP in space–time domain

- Add dynamic pseudo boundary condition for long time boundary.
- Use adaptive wavelet multilevel solver with V-cycles for BVP.
- FAS approximation to cope with nonlinear equations.
- Iterate until residual satisfies L_2 norm tolerance.
- Split space–time domain in time direction into manageable slices.

Numerical method: pseudo BVP in space–time domain

- Add dynamic pseudo boundary condition for long time boundary.
- Use adaptive wavelet multilevel solver with V-cycles for BVP.
- FAS approximation to cope with nonlinear equations.
- Iterate until residual satisfies L_2 norm tolerance.
- Split space–time domain in time direction into manageable slices.

Numerical method: pseudo BVP in space–time domain

- Add dynamic pseudo boundary condition for long time boundary.
- Use adaptive wavelet multilevel solver with V-cycles for BVP.
- FAS approximation to cope with nonlinear equations.
- Iterate until residual satisfies L_2 norm tolerance.
- Split space–time domain in time direction into manageable slices.

Numerical method: pseudo BVP in space–time domain

- Add dynamic pseudo boundary condition for long time boundary.
- Use adaptive wavelet multilevel solver with V-cycles for BVP.
- FAS approximation to cope with nonlinear equations.
- Iterate until residual satisfies L_2 norm tolerance.
- Split space–time domain in time direction into manageable slices.

Numerical method: pseudo BVP in space–time domain

- Add dynamic pseudo boundary condition for long time boundary.
- Use adaptive wavelet multilevel solver with V-cycles for BVP.
- FAS approximation to cope with nonlinear equations.
- Iterate until residual satisfies L_2 norm tolerance.
- Split space–time domain in time direction into manageable slices.

Numerical method: pseudo BVP in space–time domain

- Add dynamic pseudo boundary condition for long time boundary.
- Use adaptive wavelet multilevel solver with V-cycles for BVP.
- FAS approximation to cope with nonlinear equations.
- Iterate until residual satisfies L_2 norm tolerance.
- Split space–time domain in time direction into manageable slices.

1D+t example: Burgers equation

$$\frac{\partial u}{\partial t} + (U + u)\frac{\partial u}{\partial x} = \nu \frac{\partial^2 u}{\partial x^2}, \quad x \in (-1, 1), \ t > 0$$

- Steepening shock: $U = 0$, $u(x, 0) = -\sin(\pi x)$, $u(\pm 1, t) = 0$.
- Moving shock: $U = 1$, $u(x, 0) = -\tanh((x + 1/2)/(2\nu))$, $u(\pm\infty, t) = \mp 1$.
- Parameters: $\nu = 10^{-2}$, $\epsilon = 10^{-5}$.

1D+t example: Burgers equation

$$\frac{\partial u}{\partial t} + (U+u)\frac{\partial u}{\partial x} = \nu \frac{\partial^2 u}{\partial x^2}, \quad x \in (-1,1),\ t > 0$$

- Steepening shock: $U = 0$, $u(x,0) = -\sin(\pi x)$, $u(\pm 1, t) = 0$.
- Moving shock: $U = 1$, $u(x,0) = -\tanh((x+1/2)/(2\nu))$, $u(\pm\infty, t) = \mp 1$.
- Parameters: $\nu = 10^{-2}$, $\epsilon = 10^{-5}$.

1D+t example: Burgers equation

$$\frac{\partial u}{\partial t} + (U + u)\frac{\partial u}{\partial x} = \nu \frac{\partial^2 u}{\partial x^2}, \quad x \in (-1, 1), \; t > 0$$

- Steepening shock: $U = 0$, $u(x, 0) = -\sin(\pi x)$, $u(\pm 1, t) = 0$.
- Moving shock: $U = 1$, $u(x, 0) = -\tanh((x + 1/2)/(2\nu))$, $u(\pm\infty, t) = \mp 1$.
- Parameters: $\nu = 10^{-2}$, $\epsilon = 10^{-5}$.

1D+t example: Burgers equation

$$\frac{\partial u}{\partial t} + (U+u)\frac{\partial u}{\partial x} = \nu\frac{\partial^2 u}{\partial x^2}, \quad x \in (-1,1),\ t>0$$

- Steepening shock: $U=0,\ u(x,0)=-\sin(\pi x),\ u(\pm 1,t)=0.$
- Moving shock: $U=1,\ u(x,0)=-\tanh((x+1/2)/(2\nu)),$ $u(\pm\infty,t)=\mp 1.$
- Parameters: $\nu=10^{-2}$, $\epsilon=10^{-5}$.

Burgers equation: steepening shock

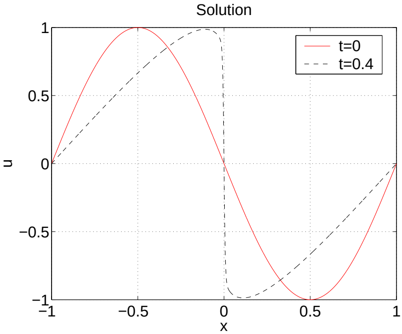

Solution

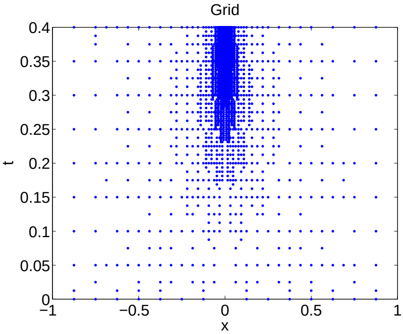

Adapted grid

Burgers equation: moving shock

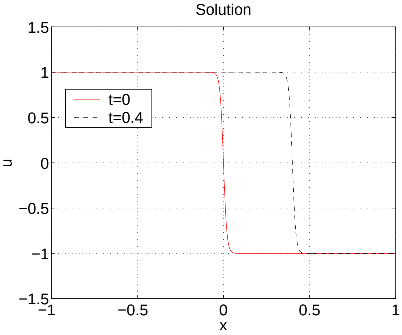

Solution

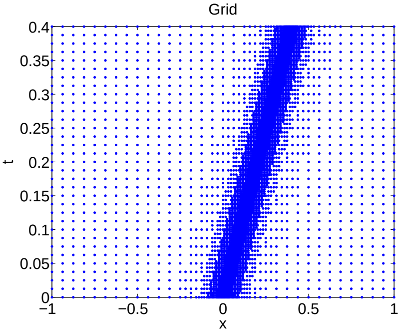

Adapted grid

Burgers equation: time integration error

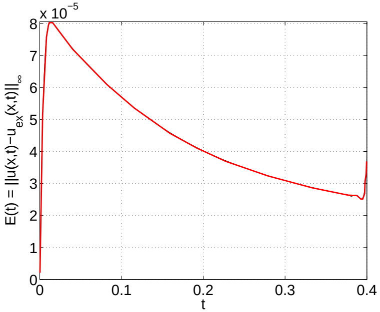

Global error in time

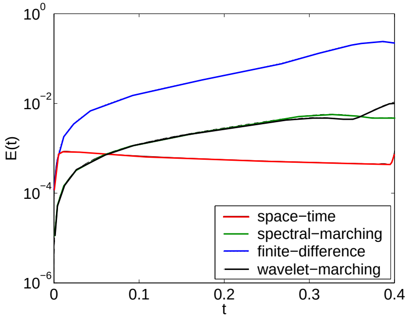

Comparison with time marching

2D decaying turbulence simulations

Run	Re	Resolution	Δx	λ	Re_λ
I	1 260	192×192	3.3×10^{-2}	1.1×10^{-1}	138
II	2 530	192×192	3.3×10^{-2}	8.3×10^{-2}	195
III	5 050	192×192	3.3×10^{-2}	5.9×10^{-2}	275
IV	10 100	256×256	2.5×10^{-2}	4.1×10^{-2}	389
V	20 200	384×384	1.6×10^{-2}	2.9×10^{-2}	551
VI	40 400	512×512	1.2×10^{-2}	2.0×10^{-2}	779

Table: Parameters for space–time turbulence simulations.

2D decaying turbulence simulations

Run	Re	Resolution	Δx	λ	Re_λ
I	1 260	192×192	3.3×10^{-2}	1.1×10^{-1}	138
II	2 530	192×192	3.3×10^{-2}	8.3×10^{-2}	195
III	5 050	192×192	3.3×10^{-2}	5.9×10^{-2}	275
IV	10 100	256×256	2.5×10^{-2}	4.1×10^{-2}	389
V	20 200	384×384	1.6×10^{-2}	2.9×10^{-2}	551
VI	40 400	512×512	1.2×10^{-2}	2.0×10^{-2}	779

Table: Parameters for space–time turbulence simulations.

Comparison simulations were also done using a standard pseudo-spectral code, and time marching adaptive wavelet simulations were done to estimate the number of spatial degrees of freedom.

$Re = 40\,400$ simulation, $t = [0, 400]$

$Re = 40\,400$ simulation, $t = [21, 128]$

Vorticity field at $Re = 40\,400$

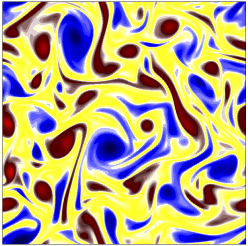

7 895 wavelet modes

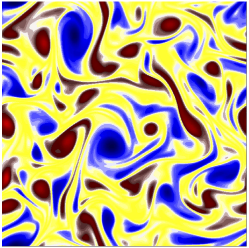

263 169 Fourier modes

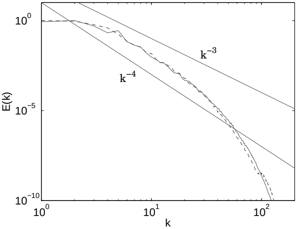

Energy spectrum

Vorticity at $t = 126$

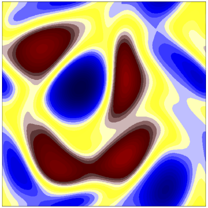

$Re = 1\,260$

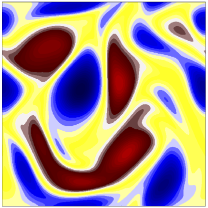

$Re = 2\,530$

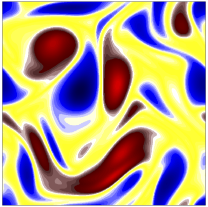

$Re = 5\,050$

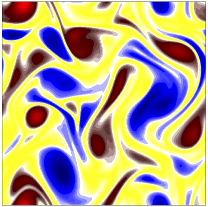

$Re = 10\,100$

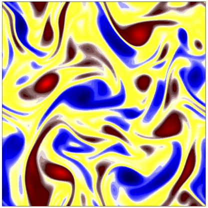

$Re = 20\,200$

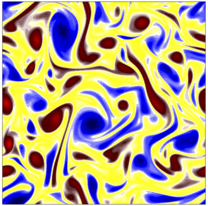

$Re = 40\,400$

Adaptive wavelet grids at $\mathrm{Re} = 40\,400$

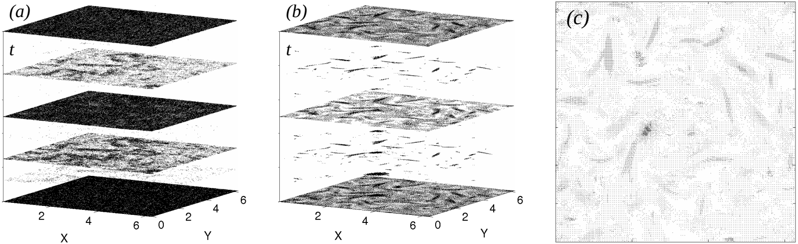

$t \in [0, 2.1]$ $t \in [123.8, 126.0]$ Spatial grid only at $t = 126.0$

Adaptive wavelet grids at $\mathrm{Re} = 40\,400$

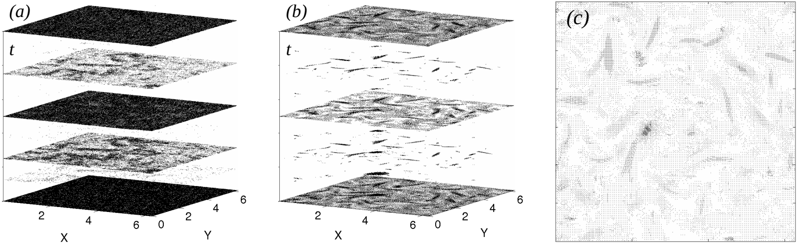

$t \in [0, 2.1]$ $t \in [123.8, 126.0]$ Spatial grid only at $t = 126.0$

Note the strong time intermittency of the solution: the smallest time step is strongly localized in space.

Scaling of modes with Reynolds number

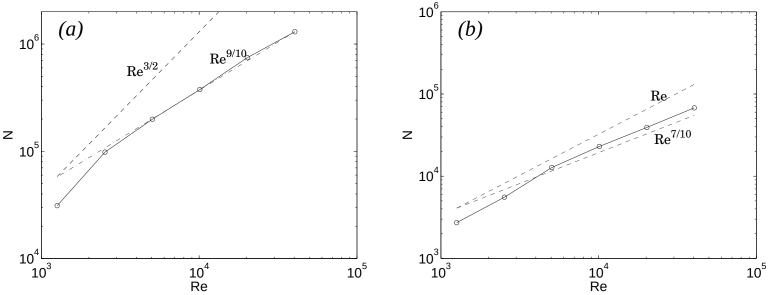

Space–time Space only

Scaling of modes with Reynolds number

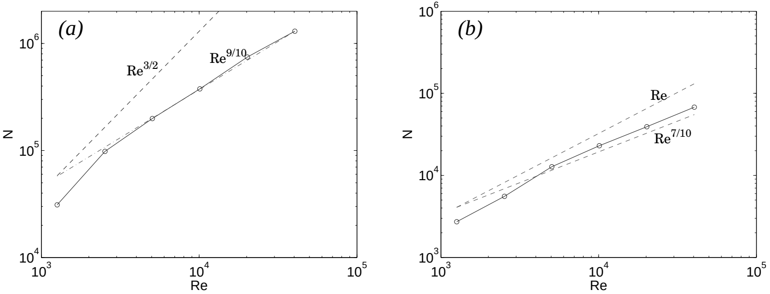

Space–time Space only

Note that intermittency reduces the number of modes significantly compared with the usual computational estimates.

β-model fractal dimension

The β-model for two-dimensional turbulence implies that the spatial modes should scale like $\mathcal{N} \sim \mathrm{Re}^{\frac{3D_F}{D_F+4}}$.

β-model fractal dimension

The β-model for two-dimensional turbulence implies that the spatial modes should scale like $\mathcal{N} \sim \mathrm{Re}^{\frac{3D_F}{D_F+4}}$.

β-model fractal dimension

The β-model for two-dimensional turbulence implies that the spatial modes should scale like $\mathcal{N} \sim \mathrm{Re}^{\frac{3D_F}{D_F+4}}$.

- Spatial fractal dimension is $\boxed{D_F \approx 1.2}$

β-model fractal dimension

The β-model for two-dimensional turbulence implies that the spatial modes should scale like $\mathcal{N} \sim \mathrm{Re}^{\frac{3D_F}{D_F+4}}$.

- Spatial fractal dimension is $\boxed{D_F \approx 1.2}$
- A simple extension gives a temporal fractal dimension $\boxed{D_F \approx 0.3}$

β-model fractal dimension

The β-model for two-dimensional turbulence implies that the spatial modes should scale like $\mathcal{N} \sim \mathrm{Re}^{\frac{3D_F}{D_F+4}}$.

- Spatial fractal dimension is $\boxed{D_F \approx 1.2}$
- A simple extension gives a temporal fractal dimension $\boxed{D_F \approx 0.3}$
- Flow appears to be much more intermittent in time

β-model fractal dimension

The β-model for two-dimensional turbulence implies that the spatial modes should scale like $\mathcal{N} \sim \mathrm{Re}^{\frac{3D_F}{D_F+4}}$.

- Spatial fractal dimension is $\boxed{D_F \approx 1.2}$
- A simple extension gives a temporal fractal dimension $\boxed{D_F \approx 0.3}$
- Flow appears to be much more intermittent in time

Assumes that the active proportion of the flow decreases like lengthscale to the power $D - D_F$.

Conclusions

- Spatial modes scale like $\mathrm{Re}^{0.7}$
- Space–time modes scale like $\mathrm{Re}^{0.9}$
- Spatial fractal dimension of active regions is 1.2
- Temporal fractal dimension is 0.3
- 2D turbulence is more intermittent than previously thought

Conclusions

- Spatial modes scale like $\mathrm{Re}^{0.7}$
- Space–time modes scale like $\mathrm{Re}^{0.9}$
- Spatial fractal dimension of active regions is 1.2
- Temporal fractal dimension is 0.3
- 2D turbulence is more intermittent than previously thought

Conclusions

- Spatial modes scale like $\mathrm{Re}^{0.7}$
  (compared with homogeneous estimate Re^1)
- Space–time modes scale like $\mathrm{Re}^{0.9}$

- Spatial fractal dimension of active regions is 1.2
- Temporal fractal dimension is 0.3
- 2D turbulence is more intermittent than previously thought

Conclusions

- Spatial modes scale like $\mathrm{Re}^{0.7}$
  (compared with homogeneous estimate Re^1)
- Space–time modes scale like $\mathrm{Re}^{0.9}$

- Spatial fractal dimension of active regions is 1.2
- Temporal fractal dimension is 0.3
- 2D turbulence is more intermittent than previously thought

Conclusions

- Spatial modes scale like $\mathrm{Re}^{0.7}$
  (compared with homogeneous estimate Re^1)
- Space–time modes scale like $\mathrm{Re}^{0.9}$
  (compared with homogeneous estimate $Re^{1.5}$)
- Spatial fractal dimension of active regions is 1.2
- Temporal fractal dimension is 0.3
- 2D turbulence is more intermittent than previously thought

Conclusions

- Spatial modes scale like $\mathrm{Re}^{0.7}$
  (compared with homogeneous estimate Re^1)
- Space–time modes scale like $\mathrm{Re}^{0.9}$
  (compared with homogeneous estimate $Re^{1.5}$)
- Spatial fractal dimension of active regions is 1.2
- Temporal fractal dimension is 0.3
- 2D turbulence is more intermittent than previously thought

Conclusions

- Spatial modes scale like $\mathrm{Re}^{0.7}$
  (compared with homogeneous estimate Re^1)
- Space–time modes scale like $\mathrm{Re}^{0.9}$
  (compared with homogeneous estimate $Re^{1.5}$)
- Spatial fractal dimension of active regions is 1.2
- Temporal fractal dimension is 0.3
- 2D turbulence is more intermittent than previously thought

Conclusions

- Spatial modes scale like $\mathrm{Re}^{0.7}$
  (compared with homogeneous estimate Re^1)
- Space–time modes scale like $\mathrm{Re}^{0.9}$
  (compared with homogeneous estimate $Re^{1.5}$)
- Spatial fractal dimension of active regions is 1.2
- Temporal fractal dimension is 0.3
- 2D turbulence is more intermittent than previously thought

Conclusions

- Spatial modes scale like $\mathrm{Re}^{0.7}$
  (compared with homogeneous estimate Re^1)
- Space–time modes scale like $\mathrm{Re}^{0.9}$
  (compared with homogeneous estimate $Re^{1.5}$)
- Spatial fractal dimension of active regions is 1.2
- Temporal fractal dimension is 0.3
- 2D turbulence is more intermittent than previously thought

This is the first quantitative estimate of the Reynolds number dependence of the space–time intermittency of turbulence